Adsorption of water on porous Vycor glass studied by ellipsometry

Alberto Álvarez-Herrero, Raquel L. Heredero, Eusebio Bernabeu, and David Levy

The variation of the optical properties of porous Vycor glass (Corning, Model 7930) under different relative-humidity conditions was studied. The adsorption of water into the glass pores was investigated with spectroscopic ellipsometry. The change of the refractive index was $\Delta n \sim 0.04$ between 5% and 90% relative humidity. A linear relation between the ellipsometer parameter tan Ψ, the amount of water adsorbed in the glass pores, and information about the pore-size distributions was established. The results are in accord with the values obtained from N_2 isotherms, transmission electron microscope micrographs, and the manufacturer's specifications (radius of $\sim$20 Å). The possibility of using this material as a transducer for implementation in a fiber-optic sensor to measure humidity was evaluated.

OCIS codes: 160.4760, 120.2130, 160.6030, 010.7340.

1. Introduction

Porous materials have been studied for several decades. They have been used for multiple applications: desiccants, membranes, and host matrices for different dopants. In particular, surface and interfacial effects that occur on silica glasses have been investigated because of their great potential for application in many technologies.

In this sense the commercially available porous Vycor glass (PVG), Corning, Model 7930, is a 96%-silica glass that has been used in many studies. The porosity and the fractal structure of this material have been widely analyzed.[1,2] PVG has also been used as a template in the growth of metals, in semiconductor–insulator composite fabrication, and as a host dielectric matrix for organic or inorganic materials.[3,4] The behaviors of vapors and fluids confined in small pores of PVG have been of great research interest[5–7] because of their perturbation effects. These factors have important implications in many areas, such as molecular diffusion in membranes, solvation forces, or colloid interactions. Because of the important role of water in most chemical and biological systems, its behavior in porous systems such as PVG has been investigated extensively.[8,9]

The behavior of the complex refractive index of porous materials with respect to the relative humidity (RH) is an attractive topic for different areas in optics: system design and manufacturing, the stability of interference filters and antireflectance coatings, and the development of new transducers for sensing. In this paper the optical properties of PVG are studied under different RH environments. In this sense the possibility of using this material as a transducer that is implemented in a fiber-optic sensor to measure RH is investigated through spectroscopic ellipsometry.[10] Ellipsometry permits the measurement of the optical properties of materials with high accuracy and precision, and this technique is useful for studying changes in the refractive index with the RH. From the variation of ellipsometric parameters information about the pore size can be also extracted. The ellipsometric results of pore-size distributions were compared with data obtained from the adsorption and the desorption of N_2 adsorbed in the PVG and from transmission electron microscope (TEM) micrographs.

A. Álvarez-Herrero (alvarez@inta.es), R. L. Heredero, and D. Levy are with the Laboratorio de Instrumentación Espacial (LINES), Área de Cargas Útiles e Instrumentación, División de Ciencias de Espacio, Instituto Nacional de Técnica Aeroespacial (INTA), 28850 Torrejón de Ardoz, Madrid, Spain. E. Bernabeu is with the Departamento de Óptica, Facultad de Ciencias Físicas, Universidad Complutense de Madrid, 28040 Madrid, Spain. D. Levy is also with the Instituto de Ciencia de Materiales de Madrid, Instituto de Ciencia de Materiales de Madrid, Consejo Superior de Investigaciones Cientificas, 28049 Cantoblanco, Madrid, Spain.

Received 22 June 2000; revised manuscript received 30 October 2000.

0003-6935/01/040527-06$15.00/0

2. Experimental Details

The PVG samples (Corning, Model 7930) that were used were first cleaned with ultrasound waves inside a glass vial filled with acetone. After this process the samples were dried at 150 °C for 1 h.

A. Optical Characterization: Spectroscopic Ellipsometry

The sample for the ellipsometry measurements consisted of a disk with a 15-mm diameter and a 3-mm thickness. Only one face of the sample was polished to achieve adequate reflectivity for the ellipsometry measurements and to avoid backreflection from the opposite face.

A rotating-polarizer spectroscopic ellipsometer[11] (SOPRA, Model ES-4G) was used to measure the refractive index of the PVG under different conditions of the RH. The ellipsometer's nominal repeatability is 0.005 for the ellipsometric parameters tan Ψ and cos Δ, and its spectral range was 400–835 nm.

A climatic chamber specially designed to be coupled to the ellipsometer was used to perform *in situ* measurements of the change in optical properties with the RH. The stability of the chamber is $\pm 1\%$ RH, and the working range is from 7% to 90% RH. Temperature and humidity inside the chamber were measured with VAISALA sensors: Model PHM 233 with probe Model HMP46 (accuracies of 0.2 °C and 1% RH).

The ellipsometric measurements were performed at two different angles. Position A corresponds to an incident angle of $55.09° \pm 0.01°$ (similar to the Brewster angle of silica), which is the optimum angle for transparent samples. For angle A the estimated systematic error was $\delta n \leq 0.002$. The RH and the temperature were 32% and 24.0 °C, respectively, for the measurements at position A. Position B corresponds to an incident angle equal to $70.11° \pm 0.01°$. All measurements with the climatic chamber were performed at this angle because at position A the errors introduced by changes in the polarization when light passes through the windows cannot be neglected. The total systematic error estimated for measurements at position B and with the climatic chamber coupled was $\delta n \leq 0.01$. The measurement repeatability was better than 0.001. We are interested in relative changes in the optical properties of the PVG with the RH, so the systematic errors are not important for our purpose.

B. Characterization by Use of a Surface-Area Analyzer and a Transmission Electron Microscope

To compare the ellipsometric results, we used a Model ASAP 2010 accelerated surface-area analyzer from Micromeritics[12] for measurements of the surface area and the porosity. The pore-size distribution was obtained from N_2 adsorption–desorption isotherms at 77 K. The PVG samples were outgassed at 150 °C for 24 h.

Microstructural observations of the Vycor samples were performed in a Philips Model CM20 (200-kV) TEM. The samples were crushed in a dilute methanol solution that eventually evaporates. The resulting particles were dispersed onto a nickel microscope carbon-holed grid.

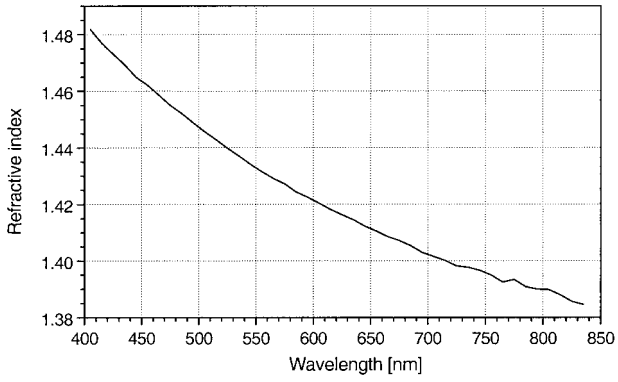

Fig. 1. Refractive index n of the Vycor sample measured at an incident angle of 55.09° for wavelengths from 400 to 835 nm with a RH of 32% and a temperature of 24 °C.

3. Experimental Results and Discussion

A. Ellipsometric Characterization

Accurate measurements of the PVG optical properties were obtained by ellipsometry at position A without the climate chamber. A rigorous model for calculating the refractive index from the ellipsometric angles Ψ and Δ should consider some degree of surface roughness and a certain inhomonegity because the amount of water adsorbed near the external surface is greater than that adsorbed inside the sample.[13] However, all the values for refractive indices in this study were obtained under the assumptions that the PVG is an isotropic and a bulk material and that its surface is not rough to simplify all the calculations. Figure 1 shows the result of the refractive-index measurement at position A.

The changes in the refractive index with the RH are shown in Fig. 2. These measurements were carried out at position B. Adsorption of the water molecules on the walls of the pores and capillary condensation occur when the RH of the environment

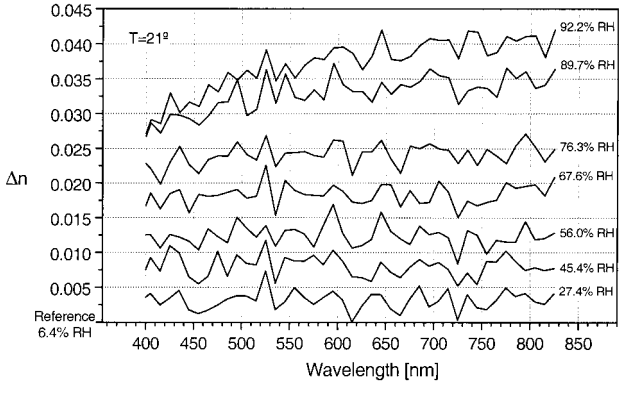

Fig. 2. Change in the value of the refractive index n with the RH. The plots show values for a wavelength range of 400–835 nm. The reference was taken at a RH of 6.4%.

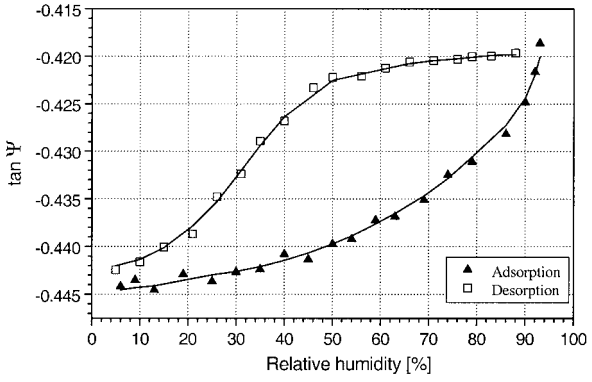

(a)

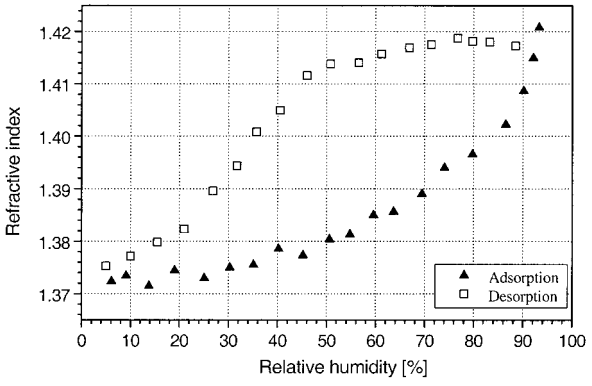

(b)

Fig. 3. Adsorption (▲) and desorption (□) isotherms of ellipsometric measurements. The temperature inside the climatic chamber was 23.1 °C: (a) The value of tan Ψ versus the RH. The plot was smoothed (solid curve) to permit the calculation of the pore-size distribution shown in Fig. 5. (b) The value of the refractive index n plotted versus the RH.

increases. The pores of the PVG fill with water, and therefore the effective refractive index increases too. The change in the refractive index is as high as $\Delta n = 0.04$ in a range between 6% and 92% RH (Fig. 2). These high variations in the optical constants could be used to develop an optical sensor head.

The possibility of using PVG for sensing purposes was examined by means of carrying out a more detailed study of the behavior of this material. One adsorption and desorption cycle of water vapor at position B was analyzed by ellipsometry at 835 nm. This wavelength was selected because it lies in the first window for sensor systems that are based on fiber optics. Figures 3(a) and 3(b) show the adsorption and the desorption isotherms, respectively, that were obtained at 23.1 °C ± 0.8 °C. In Fig. 3(a) the ellipsometric parameter tan Ψ plotted versus the RH is represented; Fig. 3(b) shows the refractive index plotted versus the RH. The shapes of both plots are similar because both of the magnitudes represented are approximately proportional to the amount of water adsorbed, as is shown below.

The curves shown in Fig. 3 present a hysteresis loop. This is a typical behavior of mesoporous materials (i.e., materials with pore widths between 2 and 50 nm) that corresponds to isotherm types IV and V, according to the Brenauer–Deming–Deming–Teller classification.[14] The type V isotherm is characterized by convexity starting at the origin toward the relative pressure axis because of the weak gas–solid interactions in which the adsorbate–adsorbate forces predominate. Otherwise, the type IV isotherm is concave for low pressures and has a point of inflection because the strongest interactions are adsorbent–adsorbate. The Brunauer–Emmett–Teller model[15] introduces the parameter c, which is related to the net heat of adsorption. The isotherms have an inflection point when $c > 2$ (type IV isotherm), which is close to the point at which the amount adsorbed is equal to the Brunauer–Emmett–Teller monolayer capacity. When $0 < c < 2$, the curve does not have a inflection point, and the plot is a type V isotherm. For more details see Ref. 16.

The curves shown in Figs. 3(a) and 3(b) have the shape of a type V isotherm because these curves are convex for low pressures. Besides, the fact that the water molecules are polar—and therefore the forces between them may be stronger than the adsorbent–adsorbate forces—supports the conclusion that the data of Figs. 3(a) and 3(b) belong to the class of type V isotherms. Nevertheless, the procedure that we used only permits knowing a magnitude that is proportional to the amount of water adsorbed on the material (refractive index or Ψ) with an unknown proportional factor; hence the parameter c cannot be calculated, and the classification of the curves shown in Figs. 3(a) and 3(b) is ambiguous.

Three parts can be distinguished in Figs. 3: Part 1 is located from 0% RH to the point at which the adsorption and the desorption points coincide (to approximately 20% RH). At 20% RH the physical adsorption of water occurs on the walls of the PVG pores. Part 2 corresponds to the hysteresis of the plot. In this area adsorption and capillary condensation of the water take place. Part 3 starts at approximately 90% RH when the pores are completely filled with water and bulk condensation begins over the external surface of the solid. The saturation of the amount of water adsorbed in the desorption branch for high RH indicates this behavior. Verification of the growth of this film of water was not carried out by ellipsometry because an achromatic compensator is required as a result of the low contrast of this layer over PVG.

The refractive-index behavior of PVG versus the RH precludes the possibility of using this material for sensing because of hysteresis. Any optical sensor that is based on changes in the refractive index of this material would generate an ambiguous value for the RH.

Although we are mainly interested in the changes in the optical properties versus the humidity, it is also interesting to show that, from only the ellipsometric data, remarkable information about the structural features of PVG can be extracted.

It was mentioned above that a linear relation exists between tan Ψ and the amount of water adsorbed inside PVG pores. The Drude approximation[17] is not suitable for this case because it applies to only thin films that are adsorbed over the external surface of the solid, and for PVG water is adsorbed not only on the external surface but also inside the pores. Despite this fact, this linear relation can be verified as follows: Our adsorbent–adsorbate system can be described in a simple way as a mixture of three main components: SiO_2, pores, and water. The volume fraction of SiO_2 (f_1) is a constant, and the volume fractions of the pores and the water (f_2 and f_3, respectively) change as the pores become filled. The effective refractive index n_e of the material is higher (lower) when f_3 increases (decreases) and f_2 decreases (increases) in the adsorption process, producing variations in the ellipsometer parameters tan Ψ and cos Δ. PVG is transparent in the visible region, so only the variations of tan Ψ are relevant because cos Δ equals +1 or −1. This behavior can be approximated by a first-order Taylor series:

$$\tan \Psi = \tan \Psi_0 + \frac{\partial \tan \Psi}{\partial n_e} \frac{\partial n_e}{\partial f_3} \Delta f_3. \quad (1)$$

The ellipsometric parameter tan Ψ for bulk materials[18] has the well-known expression of

$$\tan \Psi(n_e, \theta) = -\frac{\cos \theta (n_e^2 - \sin^2 \theta)^{1/2} - \sin^2 \theta}{\cos \theta (n_e^2 - \sin^2 \theta)^{1/2} + \sin^2 \theta}, \quad (2)$$

where θ is the incident angle. Differentiating over n_e yields

$$\frac{\partial \tan \Psi}{\partial n_e} = \frac{2 \sin^2 \theta \cos \theta n_e}{(n_e^2 - \sin^2 \theta)^{1/2}[\cos \theta (n_e^2 - \sin^2 \theta)^{1/2} + \sin^2 \theta]^2}, \quad (3)$$

On the other hand, the Bruggeman approximation for the effective refractive index of a three-component material[15] is

$$f_1 \frac{n_1^2 - n_e^2}{n_1^2 + 2n_e^2} + f_2 \frac{n_2^2 - n_e^2}{n_2^2 + 2n_e^2} + f_3 \frac{n_3^2 - n_e^2}{n_3^2 + 2n_e^2} = 0, \quad (4)$$

where n_1, n_2, and n_3 are the refractive indices of SiO_2, the pores, and the water, respectively. Equation (4) can be also written as

$$a_3 x^3 + a_2 x^2 + a_1 x + a_0 = 0, \quad (5)$$

where

$$\begin{aligned} a_0 &= n_1^2 n_2^2 n_3^2, \\ a_1 &= n_1^2 n_2^2 (2 - 3f_3) + n_1^2 n_3^2 (2 - 3f_2) + n_2^2 n_3^2 (2 - 3f_1), \\ a_2 &= 2[n_1^2 (3f_1 - 1) + n_2^2 (3f_2 - 1) + n_3^2 (3f_3 - 1)], \\ a_3 &= -4. \end{aligned} \quad (6)$$

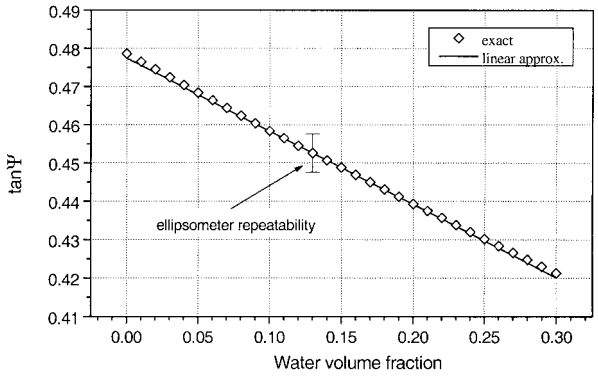

Fig. 4. Plot of tan Ψ versus the water volume fraction. Both the exact values and a linear approximation are shown. Note that the deviation between the plots is less than the repeatability of the ellipsometer (0.005).

If one takes into account that f_1 is a constant, $f_2 = 1 - f_1 - f_3$, and differentiating Eq. (5) over f_3, results in

$$\frac{\partial n_e}{\partial f_3} = \frac{3n_e(n_3^2 - n_2^2)(2n_e^2 + n_1^2)}{2(12n_e^4 - 2a_2 n_e^2 - a_1)}. \quad (7)$$

Substituting Eqs. (7) and (3) into Eq. (1) yields the linear relation between tan Ψ and f_3. To verify the accuracy of this approximation, we compared the values of tan Ψ versus f_3 from the exact expression with the values calculated from the linear approximation for the PVG. The SiO_2 volume fraction f_1 was chosen to be 0.70, according to manufacturer specifications. Because of the water adsorption in the PVG pores, f_3 varies from 0 to 0.30, and, consequently, f_2 varies from 0.30 to 0. The incident angle was 70.11°, and the refractive indices n_1, n_2, and n_3 at 800 nm were 1.453, 1, and 1.329, respectively. The results are shown in Fig. 4. The deviation between the plots is less than 0.002, which is lower than the repeatability of the ellipsometer (0.005). Hence it is demonstrated that the ellipsometer parameter tan Ψ is linearly related to the amount of water adsorbed. This fact is useful in the following calculations.

If one considers that tan Ψ is proportional to the amount of water adsorbed the Pierce method[14] can be used to calculate the pore-size distribution by use of the points obtained at a RH higher than 20% (when capillary condensation takes place). This method uses the increments of the amount of water that is adsorbed when the RH increases to calculate the pore-size distribution. To avoid negative increments that are due to experimental errors required that the isotherm be smoothed beforehand by the application of a fast Fourier transform filter to adsorption points and by the averaging of adjacent desorption points. It is important to note that this procedure provides only an estimate of the pore size because some factors are not taken into account.

First, the experiment was carried out without an outgassing process because we are interested in the material's behavior under normal conditions. Hence

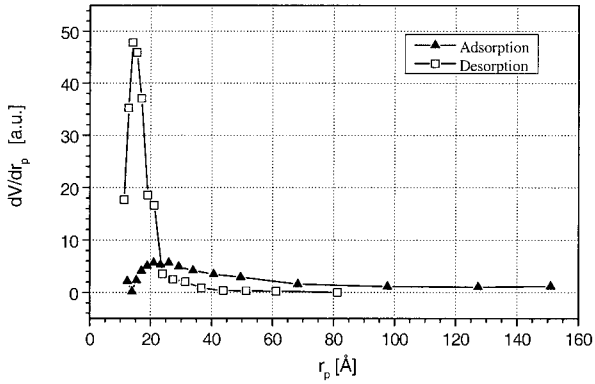

Fig. 5. Pore-size distribution calculated from the ellipsometric data [Fig. 3(a)].

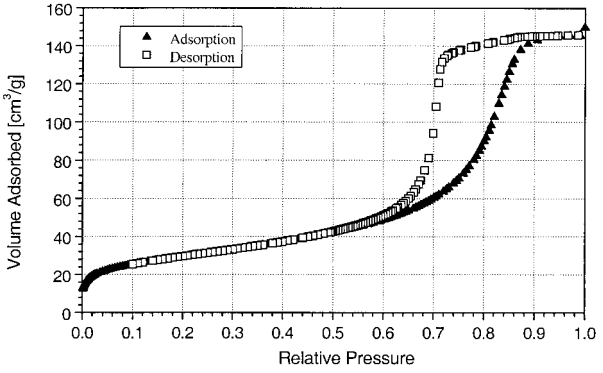

Fig. 6. Adsorption (▲) and desorption (□) isotherms of N_2 for porous Vycor glass as measured with the Model ASAP 2010 analyzer.

the walls of the pores had a layer of uncontrolled impurities. Second, the strong intermolecular forces between water molecules facilitate the growth of a multilayer during the adsorption process even though the monolayer is still incomplete on others parts of the surface. Finally, it is necessary to introduce a correction in the thickness of the growing monolayer because of the physical adsorption on the pores walls before capillary condensation takes place. The t curve for the water–Vycor glass system is not known, i.e., the statistical thickness t of the adsorbed film plotted versus the partial pressure (RH in this study). To solve this problem, we used the t curve of the N_2–Vycor system and assumed that both curves were similar. If we consider that the molecular size of N_2 and H_2O is ~0.1 nm, the difference between the t curves would be of the same order, and therefore the error introduced in the pore-size calculation for this mesoporous material will be minor at 5%.

Figure 5 shows the pore-size distributions that were calculated for the adsorption and the desorption branches, respectively. The distribution calculated from the desorption points is narrower than the one from the adsorption points because of the pores' interconnectivity.[16] The most probable pore radius obtained from the adsorption branch was 21 Å, and it was 15 Å from the desorption branch. As we show below in Subsection 3.B, the values obtained from more rigorous methods yield the same orders of magnitude for the pores. These values also agree with the specifications given by the manufacturer (~20 Å).

B. Characterization by N_2 Adsorption

An alternative method was used to compare the pore-size results obtained from the ellipsometric measurements. One adsorption–desorption cycle of N_2 was carried out with the Model ASAP 2010 analyzer. The isotherm that was obtained is shown in Fig. 6. The curve indicates a type IV isotherm, corresponding to a mesoporous material and in agreement with the ellipsometric results. A change of adsorptive (N_2 instead of water vapor) causes a change in the isotherm from type V to type IV. The adsorbent–adsorbate forces dominate the process compared with the adsorptive–adsorptive forces. The software of the Model ASAP 2010 was used to analyze the data. The algorithm utilized is an implementation of the Barrett–Johner–Halenda method.[12] It can be observed from Fig. 7 that a narrower shape of the desorption pore distribution was obtained, in accord with the distribution obtained from the ellipsometric data. The most probable pore radii obtained were 58 and 34 Å for the adsorption and the desorption branches, respectively.

Pore sizes calculated from the ellipsometric measurements are smaller than those calculated from the N_2-adsorption data. This result was expected because, in the first case, the measurements were performed under room conditions. Therefore an indeterminate amount of impurities is placed on the pores' walls, and when water adsorption occurs the effective radius of the pores is reduced. It is also necessary to note that the adsorbate–adsorbent system was different for both sets of measurements.

C. Transmission Electron Microscope Micrographs

Figure 8 shows the microstructural appearance of the Vycor samples. From the TEM micrographs, we can estimate that the radius of the pores is 50 Å, which is in accord with the Model ASAP 2010 analyzer results. Again, this value is higher than the one ob-

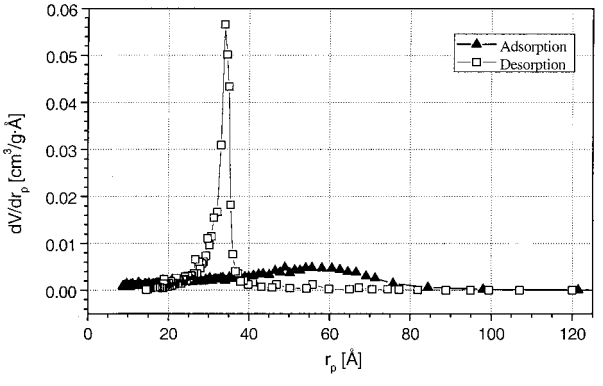

Fig. 7. Pore-size distribution calculated from the data of the N_2 isotherms.

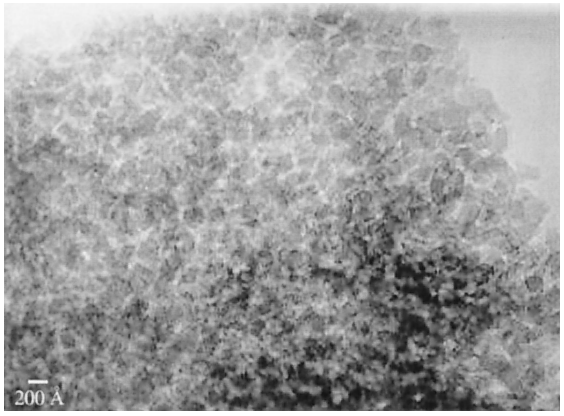

Fig. 8. TEM micrograph of the Vycor sample.

tained by ellipsometry for the same reasons mentioned in Subsection 3.B.

4. Conclusions

The behavior of the optical properties of the Model 7930 Vycor glass with the RH has been studied by ellipsometric techniques. An adsorption–desorption cycle with a hysteresis profile has been obtained, and the refractive-index changes were as high as 0.04 between 5% and 90% RH. These great variations in the refractive index could be used when considering this material as a candidate for a transducer to be integrated in a fiber-optic sensor head, but the existence of a hysteresis loop advises against this possibility.

In addition, information about the pore-size distribution has been extracted from the ellipsometric data and compared with N_2 adsorption results. The experimental curve is a typical isotherm of mesoporous materials. The mean process in these solids is the capillary condensation of adsorbate in the pores of the glass. The estimation of pore-size distributions from these data is in accord with the N_2 isotherms and the TEM micrograph results. The values obtained by ellipsometry are the lowest because of the conditions under which all the ellipsometric measurements were performed: room conditions and therefore without outgassing. We conclude that the ellipsometric technique is a useful tool for estimating the porosity of thin films when traditional methods of measuring the amount of gas adsorbed (gravimetric or volumetric methods) cannot be used.

The authors gratefully acknowledge the contribution of S. Martín Barbero for the adsorption measurements of N_2 and P. Valles González for the TEM micrographs. We are much indebted to A. Pérez Masia and A. Ruiz Paniego for enlightening discussions about adsorption in porous materials. We are grateful to H. Guerrero for his support of this study. This research has been partially supported by the Comisión Interministerial de Ciencia y Tecnología (CICYT), project ESP98-1332-C04-04.

References

1. A. Hohr, H. B. Neumann, P. W. Schmidt, P. Pfeifer, and D. Avnir, "Fractal surface and cluster structure of controlled-pore glasses and Vycor porous glass as revealed by small-angle x-ray and neutron scattering," Phys. Rev. B **38,** 1462–1467 (1988).
2. M. J. Benhan, J. C. Cook, J. C. Li, and D. K. Ross, "Small-angle neutron scattering study of adsorbed water in porous Vycor glass: supercooling phase transition and interfacial structure," Phys. Rev. B **39,** 633–636 (1989).
3. S. K. Das and R. Suryanarayanan, "Structural, optical, and electrical properties of $Pb_{1-x}Yb_xTe$ films ($0 < x < 0.25$)," J. Appl. Phys. **66,** 4843–4845 (1989).
4. M. D. Dvorak, B. L. Justus, D. K. Gaskill, and D. G. Hendersho, "Nonlinear absorption and refraction of quantum confined InP nanocrystals grown in porous glass," Appl. Phys. Lett. **66,** 804–806 (1995).
5. T. E. Huber and H. L. Tsou, "Temperature-dependent adsorption of nitrogen on porous Vycor glass," Phys. Rev. B **57,** 4991–4994 (1998).
6. T. E. Huber and C. A. Huber, "Adsorption of hydrogen on porous Vycor glass," J. Low Temp. Phys. **80,** 315–323 (1990).
7. B. Abeles, L. F. Chen, J. W. Johnson, and J. M. Drake, "Capillary condensation and surface flow in microporous Vycor glass," Isr. J. Chem. **31,** 99–106 (1991).
8. Y. Hirama, T. Takahashi, M. Hino, and T. Sato, "Studies of water adsorbed in porous Vycor glass," J. Colloid Interface Sci. **184,** 349–359 (1996).
9. P. Pissis, J. Laudat, D. Daoukaki, and A. Kyritsis, "Dynamic properties of water in porous Vycor glass studied by dielectric techniques," J. Non-Cryst. Solids **171,** 201–207 (1994).
10. Special issue on the Second International Conference on Spectroscopic Ellipsometry, Thin Solid Films **313–314** (1998).
11. *ES-4G User's Manual* (SOPRA SA., 26 rue Pierre Joigneaux, F92270 Bois-Colombes, France).
12. *ASAP 2010 Analyzer User's Manual* (Micromeritics, Norcross, Ga. 20093-1877).
13. A. Alvarez-Herrero, A. J. Fort, H. Guerrero, and E. Bernabeu, "Ellipsometric characterization and influence of relative humidity on TiO_2 layers optical properties," Thin Solid Films **349,** 212–219 (1999).
14. S. Brunauer, L. S. Deming, W. S. Deming, and E. Teller, "On a theory of the van der Waals adsorption of gases," J. Am. Chem Soc. **62,** 1723–1732 (1940).
15. S. Brunauer, P. H. Emmett, and E. Teller, "Adsorption of gases in multimolecular layers," J. Am. Chem. Soc. **60,** 309–319 (1938).
16. S. J. Gregg and K. S. W. Sing, *Adsorption, Surface Area, and Porosity* (Academic, New York, 1997).
17. H. G. Tompkins, *A User's Guide to Ellipsometry* (Academic, New York, 1993).
18. R. M. A. Azzam and N. N. Bashara, *Ellipsometry and Polarized Light* (North-Holland, Amsterdam, 1977).